

One- and Two-Electron Redox Catalysis with Lutetium Enabled by a Tris(Amido) Redox-Active Ligand

Roman G. Belli, Victoria C. Tafuri,[‡] Nicholas A. Garcia,[‡] and Courtney C. Roberts*



Cite This: *Organometallics* 2023, 42, 1059–1064



Read Online

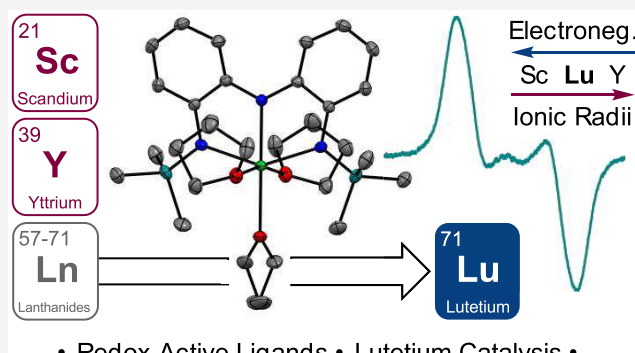
ACCESS |

Metrics & More

Article Recommendations

Supporting Information

ABSTRACT: Recently rare earth elements have been used to catalyze alkyl–alkyl cross coupling and other organic transformations. Herein we report the synthesis and characterization of a tris(amido) Lu complex, **1-Lu**, analogous to the Sc and Y rare earth complexes known to participate in these transformations. Complex **1-Lu** displays similar solid state structural properties as its Group 3 congeners, but EPR spectroscopy reveals differing behavior. **1-Lu** also was found to break the trends of reaction rates related to oxidation potential and is able to catalyze an alkyl–alkyl cross-coupling reaction faster than the Sc and Y analogs. The complex **1-Lu** was also demonstrated to participate in two-electron redox catalysis.



There has been a growing interest in exploring redox-active ligands with lanthanides and actinides because of the novel properties that these complexes exhibit.^{1–3} In particular, these complexes have applications as luminescent sensors/probes, in materials chemistry (e.g., coordination polymers, metal–organic frameworks and molecular magnets), and even in medicinal chemistry (e.g., Xcytrin, a Gd-based drug for cancer therapy that contains a texaphyrin redox-active ligand).^{4–11} Redox-active ligands have also been employed for the electro-kinetic separation of lanthanides.¹² In addition, Ln and An complexes with redox-active ligands display a myriad of reactivity ranging from redox isomerism, heterobimetallic reactivity, CO₂ reduction as well as oxidation and reduction reactions with inorganic (e.g., S₈, Se⁰) and organic (e.g., alkyl iodides) substrates.^{13–27} Redox-active ligands are also known to promote reductive elimination from An complexes as demonstrated by the radical reductive elimination of biphenyl from UBn₄ via the coordination of iminoquinone or α -diimine redox-active ligands.^{28–30}

The properties and reactivity of Group 3 metals Sc and Y is often equated with that of the lanthanides. While these metals are all rare earth elements, there can be marked differences in coordination number and the nature of metal–ligand interactions.³¹ Additionally, redox potential differences between these metals can lead to different properties.^{32,33} Our group recently reported the first example of Group 3 metals for alkyl–alkyl cross-coupling catalysis enabled by a redox-active ligand (Figure 1a).³⁴ Cross-coupling is incredibly important due to its necessity to construct molecules of medicinal importance that have C(sp³) character.^{35–40} Follow up studies correlated redox potential across different Group 3 and 4 d⁰ metals with rates of reactivity.⁴¹ We were interested if an

analogous lanthanide complex with a redox-active ligand would follow trends seen among Sc, Y, and Zr, or if the unique properties of these metals would give different results. We were also interested to see if Lu could participate in two-electron redox chemistry as was recently reported with **1-Sc** (Figure 1b).⁴² For this study, we chose to investigate lutetium since it is a diamagnetic lanthanide. Additionally, its propensity to exist as Lu(III) is similar to how Sc and Y primarily exist as M(III).⁴³ Herein we report that a tris(amido)Lu complex is an outlier among this group and actually gives the fastest rate of alkyl–alkyl cross coupling as measured with initial rates, despite having an intermediate oxidation potential. It can also participate in two-electron redox chemistry via a radical polar crossover mechanism.

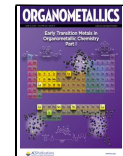
RESULTS AND DISCUSSION

Lutetium complex (NNN)Lu(THF)₃ (**1-Lu**) was prepared by addition of LuBn₃THF₃ to (NNN)H₃ in THF at $-35\text{ }^{\circ}\text{C}$, which results in the *in situ* deprotonation and metalation of the tris(amido) ligand and precursor affording (NNN)Lu(THF)₃ (**1-Lu**) as a pale yellow solid in 74% yield (Figure 2). The ¹H NMR spectrum of **1-Lu** shows four aromatic peaks and a single peak for the TMS substituents of the ligand consistent with the metalated ligand. Single crystals of **1-Lu** suitable for X-ray

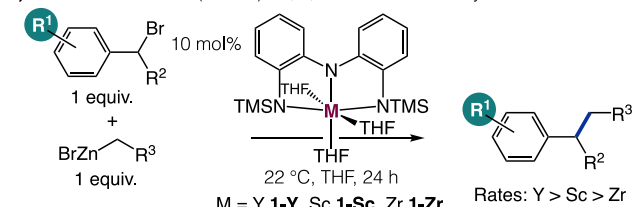
Special Issue: Early Transition Metals in Organometallic Chemistry

Received: December 31, 2022

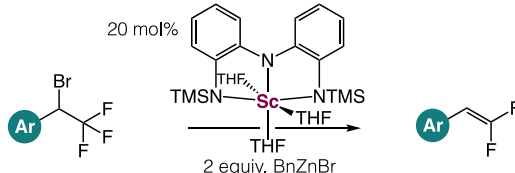
Published: February 24, 2023



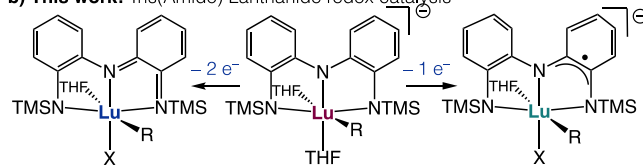
a) Previous work: Tris(Amido) Sc, Y, and Zr redox catalysis



M = Y 1-Y, Sc 1-Sc, Zr 1-Zr



b) This work: Tris(Amido) Lanthanide redox catalysis



• Can 1 and 2 electron chemistry be harnessed?

• How do reaction rates compare between lanthanides and non-lanthanides?

Figure 1. a) Previous work using tris(amido) d^0 metals as catalysts for organic transformations. b) This work demonstrating that tris(amido)Lu complexes can participate in redox catalysis.

diffraction were formed via vapor diffusion of pentane into a concentrated THF solution of **1-Lu**.

The crystal structure of **1-Lu** shows that the geometry around Lu is pseudo-octahedral with a N–Lu–N bond angle of 146.02° with respect to the terminal nitrogens of the tris(amido) ligand (Figure 2a). The C–C and C–N bond distances of the ligand are consistent with aromatic C–C bonds and C–N single bonds, which demonstrates that the ligand is in its non-oxidized, neutral state. The Lu–N bond distances range from 2.216 to 2.290 Å. Comparing **1-Lu** to the structures of our previously reported Sc (**1-Sc**) and Y (**1-Y**) analogs of **1-Lu** demonstrates that **1-Lu** has intermediate structural parameters. For example, the N–M–N bond angles decrease on the order of Sc > Lu > Y with values of $154.03(7)^\circ$, $146.02(12)^\circ$ and $143.12(7)^\circ$, respectively. In addition, the M–N bond distances increase following the trend Sc < Lu < Y with values of $2.064(2)$ – $2.157(2)$, $2.216(4)$ – $2.290(2)$ and $2.255(2)$ – $2.346(15)$ Å, respectively. These trends are consistent with the trend in the atomic radii of these metals where the atomic radius of Lu is larger than Sc, but smaller than Y. Last, the C–C and C–N bond distances of the ligand are similar when comparing the complexes with these three metals. The C–C bond distances range from $1.369(4)$ – $1.434(3)$, $1.375(3)$ – $1.433(2)$ and $1.381(5)$ – $1.436(4)$ Å for **1-Sc**, **1-Y** and **1-Lu**, respectively, indicating that the ligand is in the non-oxidized neutral state and still aromatic. The C–N bond distances range from $1.389(3)$ – $1.408(3)$, $1.395(12)$ – $1.405(2)$ and $1.388(3)$ – $1.405(4)$ Å for **1-Sc**, **1-Y** and **1-Lu**, respectively, indicating the single bond ground state character of the ligand. The similar bond distances demonstrate that changing the metal does not have a significant effect on the ligand backbone.

Complex **1-Lu** participates in one-electron chemical oxidation reactivity (Figure 2b). Addition of 0.5 equiv of PhICl_2 to **1-Lu** in $\text{THF}-d_8$ results in an immediate color

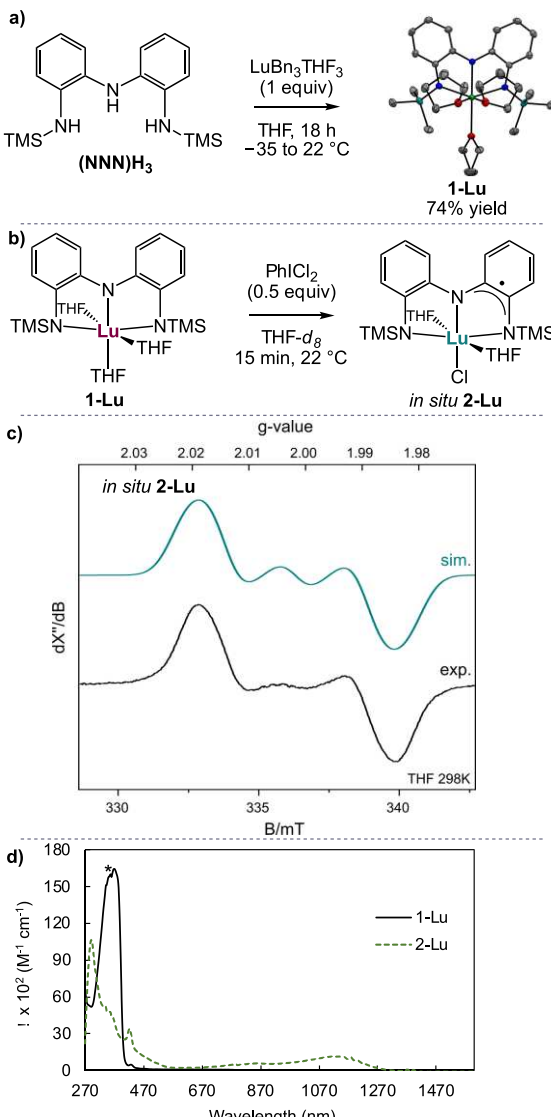


Figure 2. a) Synthesis of tris(amido) complex **1-Lu**. b) Single-electron oxidation of **1-Lu** to **2-Lu**. c) Room temperature EPR spectrum of **2-Lu**. d) UV-vis NIR spectra of **1-Lu** and **2-Lu**.

change of the solution from yellow to dark green. The ¹H NMR spectrum of this reaction mixture shows the presence of PhI, which forms when PhICl_2 acts as an oxidant, as well as a broad peak at ~ -0.5 ppm that is assigned as the TMS peak of the resulting paramagnetic complex $(\text{NNN}\bullet)\text{LuCl}(\text{THF})_2$ (**2-Lu**) (Figure S6). The X-band EPR spectrum of **2-Lu** in fluid THF at 298 K displays an anisotropic signal with $g_{x,y,z}$ values of 1.9462, 2.0039 and 2.0496, respectively (Figure 2c). Resolved hyperfine coupling to each nitrogen of the tris(amido) chelate ($A_{iso}(\text{¹⁴N}, n=2) = 67.3$ MHz); $A_{iso}(\text{¹⁴N}, n=1) = 18.5$ MHz) is observed. Interestingly, no superhyperfine coupling is observed with the ¹⁷⁵Lu nucleus ($I = 7/2$, 97.41% natural abundance). The lack of coupling from Lu contrasts the EPR spectra of previously reported **2-Sc** and **2-Y** where superhyperfine coupling to ⁴⁵Sc ($I = 7/2$, 100% natural abundance) and ⁸⁹Y ($I = 1/2$, 100% natural abundance) was observed, giving rise to some differences when a lanthanide metal is involved.⁴⁴ This contrast led us to hypothesize that potentially reactivity could be different as well. The $g_{x,y,z}$ values and lack of coupling to ¹⁷⁵Lu are consistent with **2-Lu** containing a ligand-based

radical. Complex **2-Lu** displays many charge transfer bands that span the UV–vis–NIR region (Figure 2d). A large π to π^* ligand-associated transition at $\lambda_{\max} = 295$ nm ($\epsilon = 10,370 \text{ M}^{-1} \text{ cm}^{-1}$) was observed. Ligand-dominated absorptions were observed at $\lambda = 358$ nm ($\epsilon = 4711 \text{ M}^{-1} \text{ cm}^{-1}$), 425 nm ($\epsilon = 3246 \text{ M}^{-1} \text{ cm}^{-1}$), and weaker transitions were observed at 866 nm ($\epsilon = 591 \text{ M}^{-1} \text{ cm}^{-1}$), and 1130 nm ($\epsilon = 1151 \text{ M}^{-1} \text{ cm}^{-1}$). The NIR absorptions are diagnostic for the singly oxidized form of this tris(amido) ligand, the semiquinonate oxidation state.^{41,45}

Given the chemical oxidation of **1-Lu** to **2-Lu**, we wanted to probe the electrochemical behavior of **1-Lu** to determine if multiple oxidations were feasible. The cyclic voltammogram of **1-Lu** shows two oxidation events consistent with the ability of this redox-active tris(amido) ligand to undergo two single-electron oxidations (Figure 3). The oxidation potential of the

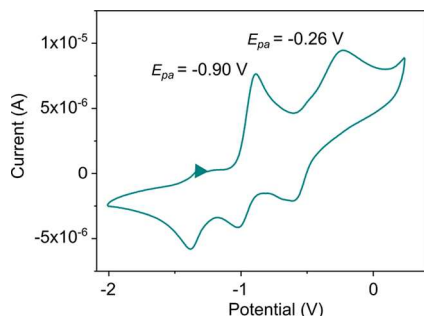


Figure 3. Cyclic voltammogram of **1-Lu** demonstrating two 1-electron oxidations.

first peak for **1-Lu** is at -0.90 V . This is an intermediate value to the first oxidation potentials of **1-Sc** (-0.77 V) and **1-Y** (-0.97 V), which produces a trend of decreasing oxidation potential of **1-Sc** $>$ **1-Lu** $>$ **1-Y**. Interestingly, this follows the trend in the electronegativity for these metals which decreases following $\text{Sc} > \text{Lu} > \text{Y}$ with values of 1.36, 1.27 and 1.22, respectively (Figure S5). This suggests that there is a relationship between the electronegativities of the metals and their influence on the oxidation potential of the ligand in these complexes. The decrease in the oxidation potentials for these three complexes also follows the trend of decreasing $\text{p}K_a$ for $[\text{M}(\text{OH}_2)_6]^{3+}$ (Figure S5). Modulation of oxidation potentials following these trends by varying the M(III) has been observed for a variety of heterobimetallic systems.^{46–48}

Given the ability of complex **1-Lu** to exhibit electrochemical properties indicating either one- or two-electron oxidation events are accessible but also knowing that there are differences in metal–ligand interactions as indicated by EPR spectroscopy, we next wanted to determine if **1-Lu** can also participate in the reported catalysis of the analogous **1-Sc** and **1-Y** complexes. We have demonstrated that an important proposed intermediate in these catalytic reactions is the electron-rich anionic benzylated complex $[(\text{NNN})\text{M}(\text{CH}_2\text{Ph})-(\text{THF})_2]^-$. The lutetium derivative of this complex $[(\text{NNN})\text{Lu}(\text{CH}_2\text{Ph})(\text{THF})_2][\text{K}]$ (**3**) was isolated in 88% yield via the addition of one equiv of benzyl potassium to **1-Lu** (Figure 4a). The ^1H and $^{13}\text{C}\{^1\text{H}\}$ NMR spectra of complex **3** display similar chemical shifts and multiplicities as our previously reported Y analog of this complex, which suggests it has a similar structure.⁴⁹ The UV–vis–NIR spectrum of complex **3** is dominated by a π to π^* ligand-associated transition at $\lambda_{\max} =$

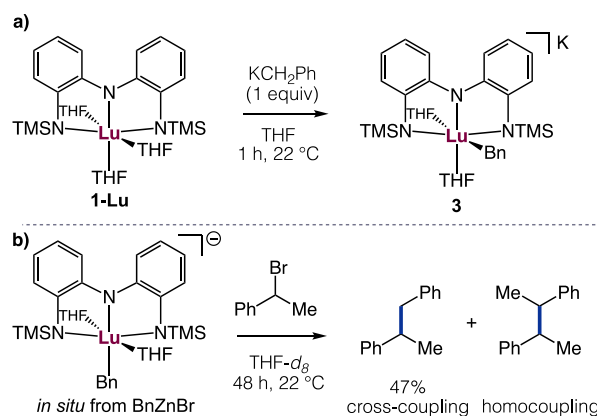


Figure 4. a) Synthesis of anionic Bn complex **3**. b) Stoichiometric cross-coupling reaction using a bromide electrophile

385 nm ($\epsilon = 19,388 \text{ M}^{-1} \text{ cm}^{-1}$) (Figure S12). Complex **1-Lu** features a small charge transfer (CT) band at $\lambda = 438 \text{ nm}$ ($\epsilon = 472 \text{ M}^{-1} \text{ cm}^{-1}$), whereas complex **3** does not exhibit this CT band. When the *in situ* generated Bn complex is exposed to 1 equiv of the electrophile 1-(bromoethyl)benzene, 47% of the cross-coupled product and near equimolar amounts of the homocoupled product are observed, demonstrating proof-of-concept for cross-coupling in a stoichiometric reaction (Figure 4b).

Complex **1-Lu** was monitored over time as a catalyst for alkyl–alkyl cross-coupling of 1 equiv of (1-bromoethyl)benzene with 1 equiv of benzyl zinc bromide affording the cross-coupled product (Figure 5). We have previously demonstrated that, for the first time, d^0 metals (Sc, Y and Zr) are able to catalyze the cross-coupling of secondary benzylic bromide electrophiles with alkyl zinc nucleophiles as enabled by a redox-active tris(amido) ligand. Experimental evidence supports that the mechanism for this reaction

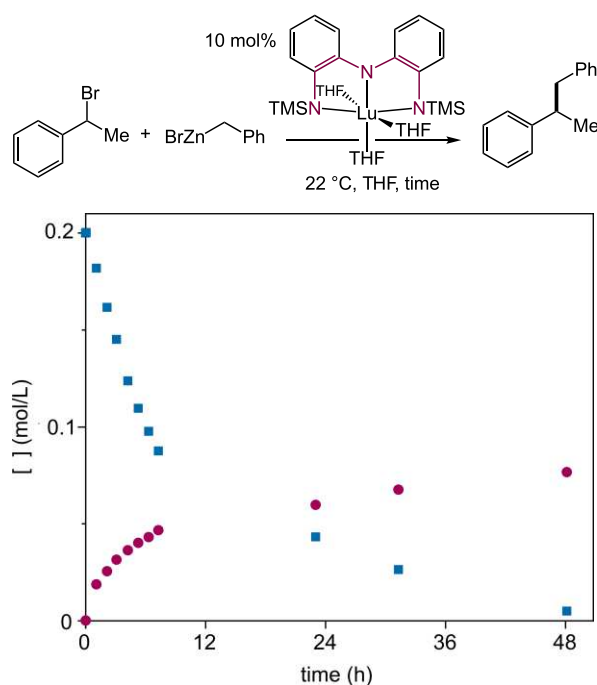


Figure 5. Reaction monitoring of consumption of electrophile (squares) for cross-coupling (circles) catalysis using **1-Lu**.

proceeds through a one-electron pathway where oxidation of the ligand by a single electron generates an alkyl radical intermediate that can participate in cross-coupling. In our previous report, we demonstrated that the oxidation potentials of these d^0 metal complexes play an important role in determining the activity for cross-coupling catalysis, where complexes with lower oxidation potentials had higher activity. Interestingly, **1-Lu** has the highest activity of all the complexes, demonstrating improved catalysis rates for Lu over non-lanthanides despite not having the lowest oxidation potential.⁴¹ The higher activity of **1-Lu** deviates from the previously reported trends seen for other d^0 non-lanthanide metals. The observed anomalous behavior demonstrates the need for studying lanthanides for C–C bond forming catalysis as the unique properties can improve catalysis.

In addition to accessing cross-coupling catalysis with these complexes via a one-electron pathway, we recently reported that the two-electron chemistry of the tris(amido) ligand in **1-Sc** is also accessible for catalysis.⁴² This was demonstrated through the ability of complex **1-Lu** to perform radical-polar crossover catalysis via the formation of *gem*-difluoroalkenes from α -CF₃ benzylic bromide substrates. The proposed mechanism for this reaction involves two sequential one-electron oxidations of the complex. The first oxidation generates a paramagnetic complex and an α -CF₃ benzylic radical. The second oxidation generates the complex with the fully oxidized redox-active ligand and converts the benzylic radical to an anion achieving the radical-polar crossover. Complex **1-Lu** is also able to catalyze the formation of a *gem*-difluorostyrene derivative through a putative radical-polar crossover (Figure 6). This was demonstrated via the synthesis

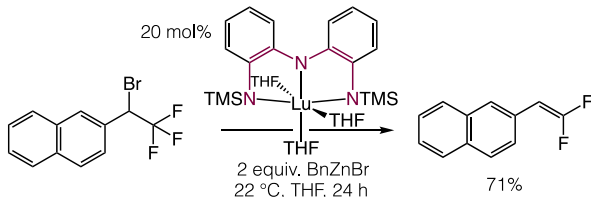


Figure 6. Formation of *gem*-difluorostyrene derivative as catalyzed by **1-Lu**.

of 2-(2,2-difluoroethyl)naphthalene from 2-(1-bromo-2,2,2-trifluoroethyl)naphthalene in 71% yield using 20 mol % of **1-Lu**. Enabled by a redox-active ligand, this allows Lu to join Ce and Sm as a lanthanide metal that can promote radical polar-crossover catalysis, although through a thermal versus photochemical method.^{50,51}

CONCLUSION

While many similarities can be drawn between the rare earth elements, their differences contribute to rich reactivity. Recently Group 3 complexes supported by tris(amido) redox-active ligands have been used to catalyze cross-coupling and other important reactions for the first time. While the same reactivity can be displayed by Lu, the activity toward cross-coupling is greater. These studies highlight the need for further investigation of lanthanides ligated by redox-active ligands for use in organic synthesis.

ASSOCIATED CONTENT

Supporting Information

The Supporting Information is available free of charge at <https://pubs.acs.org/doi/10.1021/acs.organomet.2c00673>.

Experimental details and characterization (PDF)

Accession Codes

CCDC 2227122 contains the supplementary crystallographic data for this paper. These data can be obtained free of charge via www.ccdc.cam.ac.uk/data_request/cif, or by emailing data_request@ccdc.cam.ac.uk, or by contacting The Cambridge Crystallographic Data Centre, 12 Union Road, Cambridge CB2 1EZ, UK; fax: +44 1223 336033.

AUTHOR INFORMATION

Corresponding Author

Courtney C. Roberts – Department of Chemistry, University of Minnesota, Minneapolis, Minnesota 55455, United States; orcid.org/0000-0001-8177-4013; Email: ccrob@umn.edu

Authors

Roman G. Belli – Department of Chemistry, University of Minnesota, Minneapolis, Minnesota 55455, United States; orcid.org/0000-0001-6146-670X

Victoria C. Tafuri – Department of Chemistry, University of Minnesota, Minneapolis, Minnesota 55455, United States; orcid.org/0000-0003-1486-2018

Nicholas A. Garcia – Department of Chemistry, University of Minnesota, Minneapolis, Minnesota 55455, United States; orcid.org/0000-0001-6809-2966

Complete contact information is available at:

<https://pubs.acs.org/10.1021/acs.organomet.2c00673>

Author Contributions

[‡]V.C.T. and N.A.G. contributed equally.

Notes

The authors declare no competing financial interest.

ACKNOWLEDGMENTS

Financial support for was provided by in part by the Petroleum Research Fund of the American Chemical Society (ACS PRF 62432-DNI1) and in part by NSF Award CHE-1954751. We acknowledge the Tonks, Gladfelter, and Blank groups for equipment use to obtain CV and UV-vis data. X-ray diffraction experiments were performed using a crystal diffractometer acquired through an NSF-MRI award (CHE-1229400) in the X-ray laboratory supervised by Dr. Victor G. Young,

REFERENCES

- (1) Mashima, K. Redox-Active α -Diimine Complexes of Early Transition Metals: From Bonding to Catalysis. *BCSJ*. **2020**, *93* (6), 799–820.
- (2) Galley, S. S.; Pattenade, S. A.; Ray, D.; Gaggioli, C. A.; Whitefoot, M. A.; Qiao, Y.; Higgins, R. F.; Nelson, W. L.; Baumbach, R.; Sperling, J. M.; Zeller, M.; Collins, T. S.; Schelter, E. J.; Gagliardi, L.; Albrecht-Schönzart, T. E.; Bart, S. C. Using Redox-Active Ligands to Generate Actinide Ligand Radical Species. *Inorg. Chem.* **2021**, *60* (20), 15242–15252.
- (3) Hay, M. A.; Boskovic, C. Lanthanoid Complexes as Molecular Materials: The Redox Approach. *Chemistry – A European Journal* **2021**, *27* (11), 3608–3637.

(4) Ding, B.; Solomon, M. B.; Leong, C. F.; D'Alessandro, D. M. Redox-Active Ligands: Recent Advances towards Their Incorporation into Coordination Polymers and Metal-Organic Frameworks. *Coord. Chem. Rev.* **2021**, *439*, No. 213891.

(5) Lefevre, B.; Flores Gonzalez, J.; Mattei, C. A.; Dorcet, V.; Cador, O.; Pointillart, F. Chiral or Luminescent Lanthanide Single-Molecule Magnets Involving Bridging Redox Active Triad Ligand. *Inorganics* **2021**, *9* (7), 50.

(6) Hu, J.-J.; Li, Y.-G.; Wen, H.-R.; Liu, S.-J.; Peng, Y.; Liu, C.-M. A Family of Lanthanide Metal-Organic Frameworks Based on a Redox-Active Tetrathiafulvalene-Dicarboxylate Ligand Showing Slow Relaxation of Magnetisation and Electronic Conductivity. *Dalton Trans.* **2021**, *50* (41), 14714–14723.

(7) Magda, D.; Miller, R. A. Motexafin Gadolinium: A Novel Redox Active Drug for Cancer Therapy. *Seminars in Cancer Biology* **2006**, *16* (6), 466–476.

(8) Molloy, J. K.; Jarjayes, O.; Philouze, C.; Fedele, L.; Imbert, D.; Thomas, F. A Redox Active Switch for Lanthanide Luminescence in Phenolate Complexes. *Chem. Commun.* **2017**, *53* (3), 605–608.

(9) Molloy, J. K.; Philouze, C.; Fedele, L.; Imbert, D.; Jarjayes, O.; Thomas, F. Seven-Coordinate Lanthanide Complexes with a Tripodal Redox Active Ligand: Structural, Electrochemical and Spectroscopic Investigations. *Dalton Trans.* **2018**, *47* (31), 10742–10751.

(10) Molloy, J. K.; Fedele, L.; Jarjayes, O.; Philouze, C.; Imbert, D.; Thomas, F. Structural and Spectroscopic Investigations of Redox Active Seven Coordinate Luminescent Lanthanide Complexes. *Inorg. Chim. Acta* **2018**, *483*, 609–617.

(11) Harriman, K. L. M.; Brosmer, J. L.; Ungur, L.; Diaconescu, P. L.; Murugesu, M. Pursuit of Record Breaking Energy Barriers: A Study of Magnetic Axiality in Diamide Ligated DyIII Single-Molecule Magnets. *J. Am. Chem. Soc.* **2017**, *139* (4), 1420–1423.

(12) Fang, H.; Cole, B. E.; Qiao, Y.; Bogart, J. A.; Cheisson, T.; Manor, B. C.; Carroll, P. J.; Schelter, E. J. Electro-Kinetic Separation of Rare Earth Elements Using a Redox-Active Ligand. *Angew. Chem., Int. Ed.* **2017**, *56* (43), 13450–13454.

(13) Fedushkin, I. L.; Yambulatov, D. S.; Skatova, A. A.; Baranov, E. V.; Demeshko, S.; Bogomyakov, A. S.; Ovcharenko, V. I.; Zueva, E. M. Ytterbium and Europium Complexes of Redox-Active Ligands: Searching for Redox Isomerism. *Inorg. Chem.* **2017**, *56* (16), 9825–9833.

(14) Fedushkin, I. L.; Maslova, O. V.; Morozov, A. G.; Dechert, S.; Demeshko, S.; Meyer, F. Genuine Redox Isomerism in a Rare-Earth-Metal Complex. *Angew. Chem., Int. Ed.* **2012**, *51* (42), 10584–10587.

(15) Mrutu, A.; Barnes, C. L.; Bart, S. C.; Walensky, J. R. Bringing Redox Reactivity to a Redox Inactive Metal Center – E–I (E = C, Si) Bond Cleavage with a Thorium Bis(α -Diimine) Complex. *Eur. J. Inorg. Chem.* **2013**, *2013* (22–23), 4050–4055.

(16) Kiernicki, J. J.; Higgins, R. F.; Kraft, S. J.; Zeller, M.; Shores, M. P.; Bart, S. C. Elucidating the Mechanism of Uranium Mediated Diazene N=N Bond Cleavage. *Inorg. Chem.* **2016**, *55* (22), 11854–11866.

(17) Jori, N.; Toniolo, D.; Huynh, B. C.; Scopelliti, R.; Mazzanti, M. Carbon Dioxide Reduction by Lanthanide(III) Complexes Supported by Redox-Active Schiff Base Ligands. *Inorg. Chem. Front.* **2020**, *7* (19), 3598–3608.

(18) Jori, N.; Falcone, M.; Scopelliti, R.; Mazzanti, M. Carbon Dioxide Reduction by Multimetallic Uranium(IV) Complexes Supported by Redox-Active Schiff Base Ligands. *Organometallics* **2020**, *39* (9), 1590–1601.

(19) Coughlin, E. J.; Zeller, M.; Bart, S. C. Neodymium(III) Complexes Capable of Multi-Electron Redox Chemistry. *Angew. Chem., Int. Ed.* **2017**, *56* (40), 12142–12145.

(20) Coughlin, E.; Bart, S. C. Reductive Silylation of Uranyl Mediated by Iminosemiquinone Ligands. *Polyhedron* **2019**, *170*, 783–787.

(21) Mohammad, A.; Cladis, D. P.; Forrest, W. P.; Fanwick, P. E.; Bart, S. C. Reductive Heterocoupling Mediated by Cp²U(2,2'-Bpy). *Chem. Commun.* **2012**, *48* (11), 1671–1673.

(22) Coughlin, E. J.; Qiao, Y.; Lapsheva, E.; Zeller, M.; Schelter, E. J.; Bart, S. C. Uranyl Functionalization Mediated by Redox-Active Ligands: Generation of O–C Bonds via Acylation. *J. Am. Chem. Soc.* **2019**, *141* (2), 1016–1026.

(23) Lu, E.; Liddle, S. T. Uranium-Mediated Oxidative Addition and Reductive Elimination. *Dalton Trans.* **2015**, *44* (29), 12924–12941.

(24) Wang, D.; Tricoire, M.; Cemortan, V.; Moutet, J.; Nocton, G. Redox Activity of a Dissymmetric Ligand Bridging Divalent Ytterbium and Reactive Nickel Fragments. *Inorg. Chem. Front.* **2021**, *8* (3), 647–657.

(25) Wang, D.; Moutet, J.; Tricoire, M.; Cordier, M.; Nocton, G. Reactive Heterobimetallic Complex Combining Divalent Ytterbium and Dimethyl Nickel Fragments. *Inorganics* **2019**, *7* (5), 58.

(26) Huang, W.; Diaconescu, P. L. Reactivity and Properties of Metal Complexes Enabled by Flexible and Redox-Active Ligands with a Ferrocene Backbone. *Inorg. Chem.* **2016**, *55* (20), 10013–10023.

(27) Brosmer, J. L.; Huang, W.; Diaconescu, P. L. Reduction of Diphenylacetylene Mediated by Rare-Earth Ferrocene Diamide Complexes. *Organometallics* **2017**, *36* (23), 4643–4648.

(28) Johnson, S. A.; Higgins, R. F.; Abu-Omar, M. M.; Shores, M. P.; Bart, S. C. Mechanistic Insights into Concerted C–C Reductive Elimination from Homoleptic Uranium Alkyls. *Organometallics* **2017**, *36* (18), 3491–3497.

(29) Kraft, S. J.; Fanwick, P. E.; Bart, S. C. Carbon–Carbon Reductive Elimination from Homoleptic Uranium(IV) Alkyls Induced by Redox-Active Ligands. *J. Am. Chem. Soc.* **2012**, *134* (14), 6160–6168.

(30) Matson, E. M.; Franke, S. M.; Anderson, N. H.; Cook, T. D.; Fanwick, P. E.; Bart, S. C. Radical Reductive Elimination from Tetrabenzyluranium Mediated by an Iminoquinone Ligand. *Organometallics* **2014**, *33* (8), 1964–1971.

(31) Cotton, S. A.; Raithby, P. R.; Shield, A.; Harrowfield, J. M. A Comparison of the Structural Chemistry of Scandium, Yttrium, Lanthanum and Lutetium: A Contribution to the Group 3 Debate. *Coord. Chem. Rev.* **2022**, *455*, No. 214366.

(32) Uda, T.; Jacob, K. T.; Hirasawa, M. Technique for Enhanced Rare Earth Separation. *Science* **2000**, *289* (5488), 2326–2329.

(33) Cicconi, M. R.; Le Losq, C.; Henderson, G. S.; Neuville, D. R. The Redox Behavior of Rare Earth Elements. In *Magma Redox Geochemistry*; American Geophysical Union (AGU), 2021; pp 381–398. DOI: [10.1002/9781119473206.ch19](https://doi.org/10.1002/9781119473206.ch19).

(34) Belli, R. G.; Tafuri, V. C.; Joannou, M. V.; Roberts, C. C. D0Metal-Catalyzed Alkyl–Alkyl Cross-Coupling Enabled by a Redox-Active Ligand. *ACS Catal.* **2022**, *12* (5), 3094–3099.

(35) Choi, J.; Fu, G. C. Transition Metal–Catalyzed Alkyl–Alkyl Bond Formation: Another Dimension in Cross-Coupling Chemistry. *Science* **2017**, *356* (6334), eaaf7230.

(36) Jana, R.; Pathak, T. P.; Sigman, M. S. Advances in Transition Metal (Pd,Ni,Fe)-Catalyzed Cross-Coupling Reactions Using Alkyl-Organometallics as Reaction Partners. *Chem. Rev.* **2011**, *111* (3), 1417–1492.

(37) Campeau, L.-C.; Hazari, N. Cross-Coupling and Related Reactions: Connecting Past Success to the Development of New Reactions for the Future. *Organometallics* **2019**, *38* (1), 3–35.

(38) King, A. O.; Yasuda, N. Palladium-Catalyzed Cross-Coupling Reactions in the Synthesis of Pharmaceuticals. In *Organometallics in Process Chemistry*; Brown, J. M., Fürstner, A., Hofmann, P., van Koten, G., Kündig, E. P., Reetz, M., Dixneuf, P. H., Hegedus, L. S., Knochel, P., Murai, S., Abe, A., Series Eds.; Springer Berlin Heidelberg: Berlin, Heidelberg, 2004; Vol. 6, pp 205–245. DOI: [10.1007/b94551](https://doi.org/10.1007/b94551).

(39) Lovering, F.; Bikker, J.; Humblet, C. Escape from Flatland: Increasing Saturation as an Approach to Improving Clinical Success. *J. Med. Chem.* **2009**, *52* (21), 6752–6756.

(40) Lovering, F. Escape from Flatland 2: Complexity and Promiscuity. *Med. Chem. Commun.* **2013**, *4* (3), 515–519.

(41) Belli, R. G.; Tafuri, V. C.; Roberts, C. C. Improving Alkyl–Alkyl Cross-Coupling Catalysis with Early Transition Metals through Mechanistic Understanding and Metal Tuning. *ACS Catal.* **2022**, *12* (15), 9430–9436.

(42) Gavin, J. T.; Belli, R. G.; Roberts, C. C. Radical-Polar Crossover Catalysis with a D0Metal Enabled by a Redox-Active Ligand. *J. Am. Chem. Soc.* **2022**, *144* (47), 21431–21436.

(43) Beaumier, E. P.; Pearce, A. J.; See, X. Y.; Tonks, I. A. Modern Applications of Low-Valent Early Transition Metals in Synthesis and Catalysis. *Nat. Rev. Chem.* **2019**, *3* (1), 15–34.

(44) Despite the EPR spectra of 2-Sc displaying metal coupling, spin density plots reveal the character of the radial to be 99% ligand based (see ref 34).

(45) Munhá, R. F.; Zarkesh, R. A.; Heyduk, A. F. Tuning the Electronic and Steric Parameters of a Redox-Active Tris(Amido) Ligand. *Inorg. Chem.* **2013**, *52* (19), 11244–11255.

(46) Tereniak, S. J.; Marlier, E. E.; Lu, C. C. One-Electron Ni(II)/ (I) Redox Couple: Potential Role in Hydrogen Activation and Production. *Dalton Trans.* **2012**, *41* (26), 7862–7865.

(47) Herbert, D. E.; Lionetti, D.; Rittle, J.; Agapie, T. Heterometallic Triiron-Oxo/Hydroxo Clusters: Effect of Redox-Inactive Metals. *J. Am. Chem. Soc.* **2013**, *135* (51), 19075–19078.

(48) Tsui, E. Y.; Tran, R.; Yano, J.; Agapie, T. Redox-Inactive Metals Modulate the Reduction Potential in Heterometallic Manganese–Oxido Clusters. *Nature Chem.* **2013**, *5* (4), 293–299.

(49) Attempts to cleanly synthesize the Zn variant of this complex yielded a complex, broad ^1H NMR spectrum which potentially alludes to a fluctional species where transmetalation is in equilibrium between Zn and Lu. Variable temperature NMR spectroscopy did not show decoalescence. The K species of the Y analog is well defined due to the cation-pi interactions of the cis-benzyl species. Without the presence of K, it is likely the benzyl group is trans to the amido ligand due to the differences in the NMR spectra (see page S16 and S18) (see ref 41).

(50) Pitzer, L.; Schwarz, J. L.; Glorius, F. Reductive Radical-Polar Crossover: Traditional Electrophiles in Modern Radical Reactions. *Chem. Sci.* **2019**, *10* (36), 8285–8291.

(51) Szostak, M.; Fazakerley, N. J.; Parmar, D.; Procter, D. J. Cross-Coupling Reactions Using Samarium(II) Iodide. *Chem. Rev.* **2014**, *114* (11), 5959–6039.